

Impact of the Hydrophilicity of Poly(sarcosine) on Poly(ethylene glycol) (PEG) for the Suppression of Anti-PEG Antibody Binding

Debabrata Maiti, Masayuki Yokoyama, and Kouichi Shiraishi*

Cite This: *ACS Omega* 2024, 9, 34577–34588

Read Online

ACCESS |



Metrics & More

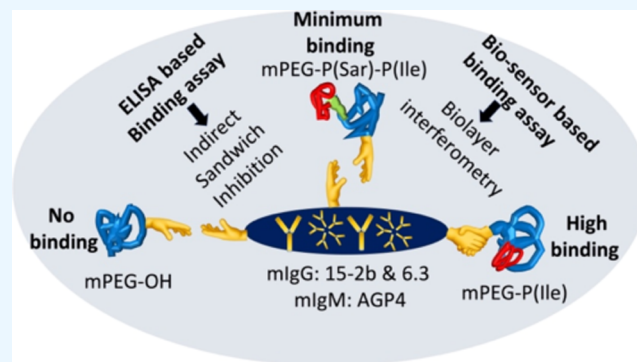


Article Recommendations



Supporting Information

ABSTRACT: A method of poly(ethylene glycol) (PEG) conjugation is known as PEGylation, which has been employed to deliver therapeutic drugs, proteins, or nanoparticles by considering the intrinsic non- or very low immunogenic property of PEG. However, PEG has its weaknesses, and one major concern is the potential immunogenicity of PEGylated proteins. Because of its hydrophilicity, poly(sarcosine) (P(Sar)) may be an attractive—and superior—substitute for PEG. In the present study, we designed a double hydrophilic diblock copolymer, methoxy-PEG-*b*-P(Sar)_{*m*} (*m* = 5–55) (mPEG-P(Sar)_{*m*}), and synthesized a triblock copolymer with hydrophobic poly(L-isoleucine) (P(Ile)). We validated that double hydrophilic mPEG-P(Sar) block copolymers suppressed the specific binding of three monoclonal anti-PEG antibodies (anti-PEG mAbs) to PEG. The results of our indirect ELISAs indicate that P(Sar) significantly helps to reduce the binding of anti-PEG mAbs to PEG. Importantly, the steady suppression of this binding was made possible, in part, thanks to the maximum number of sarcosine units in the triblock copolymer, as evidenced by sandwich ELISA and biolayer interferometry assay (BLI): the intrinsic hydrophilicity of P(Sar) had a clear supportive effect on PEG. Finally, because we used P(Ile) as a hydrophobic block, PEG-P(Sar) might be an attractive alternative to PEG in the search for protein shields that minimize the immunogenicity of PEGylated proteins.



1. INTRODUCTION

Poly(ethylene glycol) (PEG) has made significant contributions in biomedical fields including the field of targeted drug delivery owing to PEG's hydrophilic, neutral, and biocompatible properties.¹ To date, the FDA has approved several PEGylated proteins such as interferon- α 2a, interferon- α 2b, L-asparaginase, and adenosine deaminase,^{2,3} and since 1995, clinical approval has been extended to the PEGylated liposomal drugs Doxil and Onivyde.^{4,5} Even swiftly approved mRNA vaccines have used PEG-lipids in which PEG helps to stabilize lipid nanoparticles (LNPs). Various PEGylated biocompatible inorganic nanoparticles—because of their attractive physicochemical, optical, and magnetic properties—have been designed as theranostics for future clinical purposes.^{6–8}

However, as evidenced by clinical reports and animal studies, a major concern regarding the use of PEGylated biomolecules is the immunogenicity of PEG due to the generation of anti-PEG Abs, namely, anti-PEG immunoglobulin M (anti-PEG IgM) and anti-PEG immunoglobulin G (anti-PEG IgG).^{9,10} In most cases, PEGylated proteins¹¹ or PEG-liposomes¹² induce the production of anti-PEG Abs, which can effectively bind to PEGylated nanocarriers, resulting in the rapid clearance of these carriers from the body—a phenomenon commonly known as accelerated blood clearance

(ABC).^{13–15} Moreover, the binding of anti-PEG Abs to PEGylated systems triggers complement activation¹⁶ involving PEGylated liposomes,¹⁷ nanomedicines,^{18,19} and gold nanoparticles.²⁰ Recently, Ishida et al. proposed that daily use cosmetic products including soap, shampoos, toothpastes containing PEG or PEGylated derivatives are the probable sources of pre-existing anti-PEG antibodies in many healthy individuals.^{21,22} Importantly, the pre-existing anti-PEG antibodies may cause mild allergic or life-threatening anaphylactic reactions, as well as reduce the therapeutic efficacy and pharmacokinetics of PEGylated drugs.^{23–25} Therefore, minimization of the binding behaviors of anti-PEG Abs has been considered an essential topic in the current chemistry, biochemistry, and medicinal chemistry research fields.

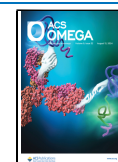
Hence, in order to overcome such limitations of PEG, it is encouraged to use hydrophilic polymers as a PEG alternative.^{26,27} In current decay, zwitterionic polymers have been

Received: March 18, 2024

Revised: June 25, 2024

Accepted: July 3, 2024

Published: July 12, 2024



aggressively deliberated as immunosuppressive polymers. For instance, zwitterionic phosphoserine polymers actively suppress undesired immune activation.²⁸ Polycarboxybetain (PCB)-modified uricase did not elicit either antiuricase or anti-PCB antibodies upon 3 weeks postinjection in a rat model.²⁹ Likewise, trimethylamine-*N*-oxide (TMAO)-derived polymer (PTMAO)-conjugated fibrinogen exhibited minimal immunogenicity.³⁰ Interestingly, the structural property of hydrophilic polymers plays an attractive role in several physiological phenomena, such as a helical L-P(EG₃Glu)-conjugated interferon (IFN) elicited a significantly milder immune response than those of coiled P(EG₃Glu) or PEG.³¹ Moreover, branched PEG or polyglycerol plays a role in the weakened ABC phenomenon.^{32,33} Furthermore, sulfoxide-containing hydrophilic polymer-coated nanoparticles have huge potential in pharmacokinetics.³⁴

Recently, Yuan et al. demonstrated that the hydrophobicity in hydrophilic polymers affects the immunogenicity of polymer–protein conjugates.³⁵ By contrast, PEG, by itself, possesses a bioinert nature characterized by hydrophilicity and flexibility.³⁶ In the present study, we focus on how the hydrophilic nature of PEG can be duplicated in PEG-conjugated polymers in order to minimize the binding of anti-PEG mAbs to PEG. Interestingly, our previous attempt to suppress anti-PEG IgM binding to hydrophilic poly(aspartic acid)-inserted PEG-*b*-poly(aspartic acid)-*b*-poly(L-phenylalanine) triblock copolymers was a successful indication of the positive impact that the insertion of hydrophilic polymers into a PEG-hydrophobic diblock copolymer occurred.³⁷ Hydrophilicity is a physicochemical property that lowers the immunogenicity of polymeric micelles. For instance, we have shown that PEG-shell (PEG-P(Lys-DOTA-Gd)) micelles with a hydrophilic inner core did not induce an anti-PEG-IgM response, whereas PEG-shell (PEG-PBLA) micelles possessing a hydrophobic inner core induced just such a response.³⁸ Therefore, the presence of hydrophobic segments neighboring hydrophilic PEGs is a potential malefactor in anti-PEG Abs responses. However, minimizing the binding of anti-PEG Abs to PEG is an enormously challenging goal. In tackling this challenge, we have focused on the important role of a hydrophilic spacer between PEG and a hydrophobic block and selected P(Sar) as a hydrophilic polymer, owing mainly to its nonionic, hydrophilic, highly biocompatible, and potentially biodegradable properties.^{39,40} The hydrophilic nature of P(Sar) has earned the polymer a reputation as a possible PEG alternative,⁴¹ drug carrier,⁴² and component in nanoparticle encapsulation.⁴³ In this respect, P(Sar) has been mentioned as a PEG alternative for protein conjugation.⁴⁴

In this study, we have designed a double hydrophilic diblock copolymer, methoxy-PEG-*b*-P(Sar)_{*m*} (*m* = 5–55) (mPEG-P(Sar)). We used a 12 kDa molecular weight PEG for the copolymer, which was conjugated with a hydrophobic polymer, poly(L-isoleucine) (P(Ile)), to prepare a triblock copolymer: mPEG-P(Sar)-P(Ile). Using gel permeation chromatography (GPC) analysis, we examined the effect that the hydrophilicity of P(Sar) in the mPEG-P(Sar)-P(Ile) would have on the aggregation of triblock copolymers. Importantly, as demonstrated by enzyme-linked immunoassay (ELISA), and biolayer interferometry (BLI) assay, P(Sar) helped to minimize the binding of various monoclonal anti-PEG Abs (anti-PEG mAbs) to PEG. Among these anti-PEG mAbs are terminal methoxy-specific anti-PEG mIgG (mIgG antibody 15–2b), PEG main-chain-specific mIgG (mIgG antibody 6.3), and PEG

main-chain-specific mIgM (mIgM antibody AGP4). We assume that P(Sar), being a hydrophilic polymer, would help to keep PEG outlying from the hydrophobic block, P(Ile) in mPEG-P(Sar)-P(Ile) triblock copolymers, and in so doing, would suppress the binding of PEG with the three aforementioned types of antibodies. Thus, in our goal of enhancing the suppression of antibody binding, we focused on triblock copolymers featuring higher numbers of sarcosine. Furthermore, hydrophilic mPEG-P(Sar) acted as mPEG toward anti-PEG mAbs, as evidenced by their similar inhibition property, indicating that mPEG-P(Sar) is in a race to replace PEG.

2. MATERIALS AND METHODS

2.1. Chemicals and Instruments. From Kanto Chemicals (Japan), we purchased isoleucine, triphosgene, dehydrated ethyl acetate (reagent grade, Wako), dehydrated tetrahydrofuran (THF, reagent grade, Wako), dehydrated *n*-hexane (reagent grade, Wako), potassium hydroxide (Wako), *n*-hexane (Wako), sulfuric acid, 3,3',5,5'-tetramethylbenzidine (TMB), and hydrogen peroxide. Likewise, we purchased α -methoxy- ω -aminopropyl-poly(ethylene glycol) (mPEG-NH₂, *M*_w = 12 kDa) from the NOF Corporation (Japan). Deuterium solvents and bovine serum albumin (BSA) were purchased from Sigma-Aldrich (Japan). *N,N*-Dimethylformamide (DMF, reagent grade and high-performance liquid chromatography (HPLC) grade), dehydrated dichloromethane (DCM, reagent grade), and lithium bromide were purchased from Fujifilm Wako Pure Chemical Corporation (Japan). Dulbecco's phosphate-buffered saline (D-PBS (–), absence of Ca/Mg) was purchased from Nakarai Tesque (Japan). Three types of anti-PEG monoclonal antibodies—mIgM antibody 15–2b, mIgG antibody 6.3, and mIgM antibody AGP4—were purchased from Academia Sinica (Taiwan). Horseradish peroxidase (HRP)-conjugated protein A/G and antimouse IgM were purchased from Bethyl Laboratories. Biotinylated mouse anti-PEG IgG and HRP-labeled streptavidin were purchased from Abcan (ab53449) and Thermo Scientific. ELISA plates were purchased, Thermo Fischer Scientific (Product code): 445101. ¹H NMR spectra were recorded on an Agilent UNITY INOVA 400 MHz NMR spectrometer. Fourier transform infrared (FTIR) spectra were analyzed with the assistance of FTIR spectroscopy (FT-IR 4100, JASCO Corporation, Japan) over the 4000–400 cm^{–1} wavenumber range. To perform GPC measurements, we relied on an HPLC system (LC 2000 series, JASCO Corporation, Japan) equipped with either a TSK-gel G4000-PW_{XL} column (eluent = D-PBS, flow rate = 1.0 mg/mL, detector = refractive index (RI)) or a TSK-gel α -3000 column (eluent = 10 mM LiBr containing DMF, flow rate = 1.0 mg/mL, detector = RI). To determine molecular weights, we performed calibration in line with polystyrene standards.

2.2. Synthesis of Isoleucine-*N*-carboxyanhydride (Ile-NCA). An L-isoleucine crystal (5.0 g, 38.1 mmol) was poured into a 500 mL two-neck round-bottom flask and dried *in vacuo* for 2 h. Then, 240 mL of a dehydrated ethyl acetate solvent was added to the crystal under a flow of N₂. Triphosgene (4.89 g, 16.5 mmol) was dissolved in 20 mL of dehydrated ethyl acetate under a flow of N₂. The triphosgene solution was added to the L-isoleucine solution under a flow of N₂. The reaction was carried out at 40 °C for 16 h under a flow of N₂. A colorless transparent solution with a small amount of the white precipitate was obtained. The reaction mixture was filtered into another 500 mL two-neck round-bottom flask under a flow of

N₂. In evaporating the solvent, we obtained a lightly yellowish viscous liquid, which we promptly dissolved in 20 mL of dehydrated THF. Then, the solution was dropwise added into 180 mL of *n*-hexane at 0 °C under vigorous stirring to obtain a precipitate. The obtained white precipitate was filtered and dried *in vacuo* (2.42 g). The transparent filtrate solution was kept at −30 °C overnight to obtain crystals (1.40 g). The dried white powder was dissolved in dehydrated THF (15 mL), followed by an addition of *n*-hexane (4 mL) at 40 °C and kept at −30 °C overnight to obtain a crystal (1.00 g). The yield (%) of the crystal was calculated to be ~48%. ¹H NMR (400 MHz, DMSO-*d*₆): δ (ppm) 9.08 (s, NH), 4.30–4.05 (br m, CH, isoleucine main chain), 1.78 (s, CH, isoleucine backbone), 1.31–1.21 (d, CH₂, isoleucine backbone), and 1.00–0.8 (br m, 2CH₃, isoleucine).

2.3. Synthesis of Sarcosine-*N*-carboxyanhydride (Sar-NCA). We synthesized Sar-NCA with slight modifications.⁴⁵ Sarcosine (5.0 g, 56.1 mmol) was dried *in vacuo* for 2 h, followed by an addition of 75 mL of dehydrated THF under a flow of N₂. Triphosgene (7.21 g, 24.3 mmol) in a dehydrated THF solution was added to the sarcosine solution. The reaction was carried out at 40 °C for 3 h under a flow of N₂. The colorless transparent solution was filtered, and the solvent was evaporated to obtain a lightly yellowish viscous liquid dissolved in dehydrated THF (100 mL). Then, 20 mL of dehydrated *n*-hexane was dropwise added under vigorous stirring at 40 °C and kept at −30 °C overnight to develop the crystal. The crystal was filtered and dried (~2.00 g). The obtained light brown crystal was purified by sublimation. The final crystal yield (%) was calculated to be ~40%, and the yield (%) of sublimation was ~60%. ¹H NMR (400 MHz, DMSO-*d*₆): δ (ppm) 4.30–4.00 (br m, CH₂, Sar backbone), and 3.10–2.85 (br m, CH₃, Sar side chain) (Figure S1).

2.4. Synthesis of mPEG-*b*-P(Sar)_{*n*} (*n* = 5–55). In synthesizing mPEG-P(Sar)s, we used a solvent consisting of dehydrated DCM and dehydrated DMF with a 1:5 (v/v) ratio. First, in a Schlenk tube, we added mPEG-NH₂ (1.00 g, 0.083 mmol) followed by DCM at room temperature under N₂. Then, we added a DMF solution of Sar-NCA (74.0 mg, 8.3 × 10^{−1} mmol) and carried out the reaction at 40 °C for 5 h. Using FTIR spectroscopy, we monitored the consumption of Sar-NCA at 1778 and 1854 cm^{−1} of C=O of the NCA (Figure S2). The obtained polymer was precipitated in cold diethyl ether, and the precipitate was dried under a vacuum (1.02 g). Table S1 summarizes the parameters involved in this reaction. All other mPEG-*b*-P(Sar)s were synthesized according to a similar method: ¹H NMR (400 MHz, CDCl₃ with TFA (0.5%, v/v)): δ (ppm) 4.30–4.00 (br m, CH₂, P(Sar) backbone), 3.85–3.35 (br m, CH₂, PEG backbone), 3.40–3.35 (s, terminal OCH₃), and 3.10–2.85 (br m, CH₃, P(Sar)) (Figure S3).

2.5. Synthesis of mPEG-*b*-Poly(isoleucine). For the synthesis of mPEG-*b*-poly(isoleucine) block copolymers (mPEG-P(Ile)s), we used a solvent consisting of dehydrated DCM and dehydrated DMF with a 1:5 (v/v) ratio. First, into a Schlenk tube, we poured mPEG-NH₂ (1.00 g, 8.3 × 10^{−2} mmol) followed by DCM at room temperature under N₂. Then, we added a DMF solution of Ile-NCA (130.3 mg, 0.83 mmol) and carried out the reaction at 40 °C for 5 h. Using FTIR spectroscopy, we monitored the consumption of Ile-NCA at 1786 and 1854 cm^{−1} of C=O of the NCA (Figure S4). The formed polymer was precipitated in cold diethyl ether and then dried under a vacuum (0.81 g). Table S2 summarizes

the parameters involved in the reaction. ¹H NMR (400 MHz, CDCl₃ with TFA (0.5%, v/v)): δ (ppm) 4.30–4.05 (br m, CH, isoleucine backbone), 3.85–3.35 (br m, CH₂, PEG backbone), 3.40–3.35 (s, PEG terminal OCH₃), 3.10–2.85 (br m, CH₃, isoleucine side chain), and 1.00–0.7 (br m, 2 CH₃, isoleucine) (Figure S5).

2.6. Synthesis of mPEG-P(Sar)-P(Ile). For the synthesis of mPEG-P(Sar)-P(Ile)s, we used a solvent consisting of dehydrated DCM and dehydrated DMF with a 1:5 (v/v) ratio. First, to a Schlenk tube, mPEG-P(Sar) (0.20 g, 1.56 × 10^{−2} mmol) was added, followed by DCM at room temperature under N₂. Then, we added a DMF solution of Ile-NCA (24.5 mg, 15.6 × 10^{−2} mmol) and carried out the reaction at 40 °C for 22 h. Using FTIR spectroscopy, we monitored the consumption of Ile-NCA at 1786 and 1854 cm^{−1} of C=O of the NCA. The obtained polymer was precipitated in cold diethyl ether, and the precipitate was dried under a vacuum (0.196 g). Table S3 summarizes the parameters involved in the reaction. ¹H NMR (400 MHz, CDCl₃ with TFA (0.5%, v/v)): δ (ppm) 4.30–4.05 (br m, CH, isoleucine backbone), 3.85–3.35 (br m, CH₂, PEG backbone), 3.40–3.35 (s, PEG terminal OCH₃), 3.10–2.85 (br m, CH₃, isoleucine side chain), and 1.00–0.7 (br m, 2CH₃, isoleucine) (Figure S6).

2.7. GPC Measurements. GPC measurements were performed at a sample concentration of 1.5 mg/mL in 10 mM LiBr containing DMF at 40 °C or at a sample concentration of 1.5 mg/mL in D-PBS (−) at 40 °C. Sample solutions were filtered before measurements.

2.8. CMC Determination. Different concentrations (4 × 10^{−7}–3 × 10^{−4} M) of mPEG-P(Ile) or mPEG-P(Sar)-P(Ile) were prepared in 4.0 mL of D-PBS (−). Then, 5 μL of an acetone solution of pyrene (5 × 10^{−4} M) was added to the polymer solutions and stirred overnight at RT (pyrene final concentration = 6 × 10^{−7} M). The solutions were excited at 319 nm (λ_{ex}) to obtain emission in the range between 360 and 400 nm with the slit width set to 5 and 5 nm for both excitation and emission. The ratio of fluorescence (FL) intensities, I₃₈₃/I₃₇₂, of the emission peaks, λ_{em} = 383 and λ_{em} = 372, was plotted against concentration to determine the CMC.

2.9. Indirect ELISA. mPEG-P(Ile) and mPEG-P(Sar)-P(Ile) were separately dissolved in ethanol (99.5%) and then prepared in a water–ethanol solvent (1:1, v/v) at various concentrations (10^{−10}–10^{−4} M). The as-prepared solutions were plated on a 96-well plate (100 μL/well) and kept overnight at 4 °C. Then, the solutions were removed, and the plate wells were washed with a wash solution (50 mM tris-buffered saline (TBS), pH = 8.0) 3 times. Since TWEEN as a surfactant in the buffer is commonly used in ELISA and contains PEG,^{31,46} therefore, we should use [3-(3-cholamidopropyl)dimethylammonio]-1-propanesulfonate, (CHAPS) instead.

Moreover, usually, CHAPS is used to exclude undesired bindings from sera. Since our current study used a simple system, which contained only monoclonal antibodies and immobilized PEGs, we used TBS as a washing solution. We blocked the plate wells with a blocking buffer solution (1% BSA in 50 mM tris-buffered saline, pH = 8.0) for 1 h at room temperature (RT) by subsequently washing 3 times with a wash solution. Then, freshly prepared antibody (mIgG antibody 15–2b, mIgG antibody 6.3, and mIgM antibody AGP4) solutions in D-PBS(−) at a concentration of 0.2 μg/mL were added to each well (100 μL/well) for 1 h, followed by

Table 1. Analytical Results for PEG-P(Sar)

polymer	feed	DP	yield (%)	$M_n \times 10^{-4a}$ (NMR)	$M_n \times 10^{-4b}$ (GPC)	M_w/M_n (g mol ⁻¹)
mPEG-NH ₂				1.20	1.68	1.05
mPEG-P(Sar)5	5	5	91	1.23	1.92	1.05
mPEG-P(Sar)10	10	10	94	1.27	1.95	1.05
mPEG-P(Sar)15	15.5	15	82	1.30	1.96	1.05
mPEG-P(Sar)40	40	40	71	1.48	1.98	1.05
mPEG-P(Sar)55	60	55	84	1.58	2.00	1.05

^aDetermined by means of ¹H NMR. ^bDetermined by means of GPC involving calibration based on polystyrene standards, with 10 mM LiBr in DMF as an eluent.

washing with a wash solution. Thereafter, 100 μ L of the as-prepared detection antibody solution of horseradish peroxidase (HRP)-conjugated protein A/G (0.02 μ g/mL) was added to each well treated with mIgG antibody 15–2b and mIgG antibody 6.3, and HRP-conjugated antimouse IgM (0.02 μ g/mL) was added to each well treated with mIgM antibody AGP4. After treatment, the plates were kept at RT for 1 h and then washed with the wash solution. TMB (100 μ L) was added to the well for 15 min, and 100 μ L of 0.36 N H₂SO₄ was added to the well to stop the reaction. The absorbance at 450 nm was recorded with a microplate reader (Multiskan GO, Thermo Fisher Scientific).

2.10. Sandwich ELISA. First, monoclonal antibody (mIgG antibody 15–2b, mIgG antibody 6.3, and mIgM antibody AGP4) solutions (2.0 μ g/mL in D-PBS (–)) were added to each well (100 μ L/well) and were kept overnight at 4 °C. The following day, the solutions were removed from the wells, which were then washed with wash solution 3 times and blocked with a blocking buffer solution for 1 h. Various concentrations (2 \times 10⁻¹⁰ to 2 \times 10⁻⁷ M) of mPEG-P(Ile), mPEG-P(Sar)-P(Ile), and mPEG-OH (M_w = 12 kDa) were separately dispersed in D-PBS and added to the plate, where they were allowed to sit for 1 h. For the detection of antibodies, we used a mixed solution of biotinylated mouse anti-PEG IgG (0.04 μ g/mL) as a detection antibody and HRP-labeled streptavidin (0.0275 μ g/mL). Biotinylated mouse anti-PEG IgG was specifically bound to PEG (main chain), which was already bound with a primary anti-PEG antibody. We prepared the solutions for approximately 30 min before adding them to the plate. The wells were washed with the wash solution 3 times before the premixed detection solutions were added to the wells (100 μ L/well). After the wells were filled with the solution, the plates were kept for 1 h at RT and were then washed with the wash solution. TMB (100 μ L) was added to each well and allowed to sit for 15 min, at which point, we stopped the reactions by adding 100 μ L of 0.36 M H₂SO₄ to the wells. The absorbance at 450 nm was recorded with a microplate reader.

2.11. Indirect ELISA for Binding of the BSA-Polymer with Serially Diluted Antibodies. A D-PBS solution of mPEG-BSA or mPEG-P(Sar)-BSA with a PEG concentration of 20 μ g/mL was immobilized onto the plate wells, and the plate wells were kept overnight at 4 °C. Then, the solutions were removed, and the plate wells were washed with the wash solution 3 times and blocked with a blocking buffer solution 1% BSA in 50 mM tris-buffered saline, pH = 8.0 (TBS), for 1 h at RT subsequent to 3 times washing with the wash solution. Then, the freshly prepared monoclonal antibody (mIgG antibody 15–2b, mIgG antibody 6.3, and mIgM antibody AGP4) solutions in D-PBS(–) with different concentrations (0.2–20.0 μ g/mL) were added to each well (100 μ L/well) for

1 h at RT, followed by washing with the wash solution. Thereafter, 100 μ L of the as-prepared detection antibody solution of HRP-conjugated protein A/G with a concentration of 0.01 μ g/mL was added to each well treated with mIgG antibody 15–2b and mIgG antibody 6.3. HRP-conjugated antimouse IgM antibody (0.01 μ g/mL) was added to each well treated with mIgM antibody AGP4. After treatment, the plate wells were kept at RT for 1 h and washed with the wash solution. TMB (100 μ L) was added to the well for 15 min, and 100 μ L of 0.36 N H₂SO₄ was added to each well to stop the reaction. The absorbance at 450 nm was recorded with a microplate reader (Multiskan GO, Thermo Fisher Scientific).

2.12. Inhibition ELISA. We prepared mPEG-poly(*b*-benzyl-L-aspartate) diblock copolymer ($M_{w,PEG}$ = 12 kDa, mPEG-PBLA)-immobilized wells according to a method we had used in previous research.³⁷ After completing the preparation, we removed the solutions from the plate wells, which were washed with the wash solution 3 times and then blocked with a blocking buffer solution for 1 h. Three types of monoclonal antibody solutions (mIgG antibody 15–2b, mIgG antibody 6.3, and mIgM antibody AGP4) were prepared at a concentration of 2.0 μ g/mL in D-PBS(–). Meanwhile, mPEG-NH₂, mPEG-P(Sar), mPEG-P(Ile), and mPEG-P(Sar)-P(Ile) were separately dissolved in D-PBS(–) at various concentrations (5 \times 10⁻¹¹ to 2 \times 10⁻⁴ M) and mixed with the as-prepared antibody solutions. The mixed solutions were added to wells (100 μ L/well) and kept for 1 h. Thereafter, 100 μ L of HRP-conjugated protein A/G (0.2 μ g/mL) was added to the mIgG antibody 15–2b-treated wells and the mIgG antibody 6.3-treated wells, and 100 μ L of an HRP-conjugated antimouse IgM antibody solution (0.2 μ g/mL) was added to the mIgM antibody AGP4-treated wells. After treatment, the plates were kept for 1 h and then washed with the wash solution. TMB (100 μ L) was added to each well and allowed to sit for 15 min, at which point, we stopped the reactions by adding 0.36 N H₂SO₄ (100 μ L) to the plate wells. The absorbance at 450 nm was recorded with a microplate reader.

2.13. Biolayer Interferometry (BLI). BLI experiments were performed on an Octet R2 system (Sartorius Inc.) at 30 °C with an orbital shake speed of 1000 rpm. Aminopropyl silane (APS) biosensors were washed with D-PBS (–) for 10 min, followed by immobilization of 5.0 μ g/mL monoclonal anti-PEG antibodies (mIgG antibody 15–2b, mIgG antibody 6.3, and mIgM antibody AGP4) for 10 min on the sensor. The anti-PEG mAbs-coated sensors were washed with D-PBS (–), followed by addition of a blocking buffer solution (0.1% BSA in 50 mM tris-buffered saline, pH = 8.0) for 5 min, and the sensor was washed with D-PBS. Different concentrations (2.5 \times 10⁻⁷–2.0 \times 10⁻⁶ M) of mPEG-P(Ile) or mPEG-P(Sar)-P(Ile) were allowed for the association with antibodies for 10

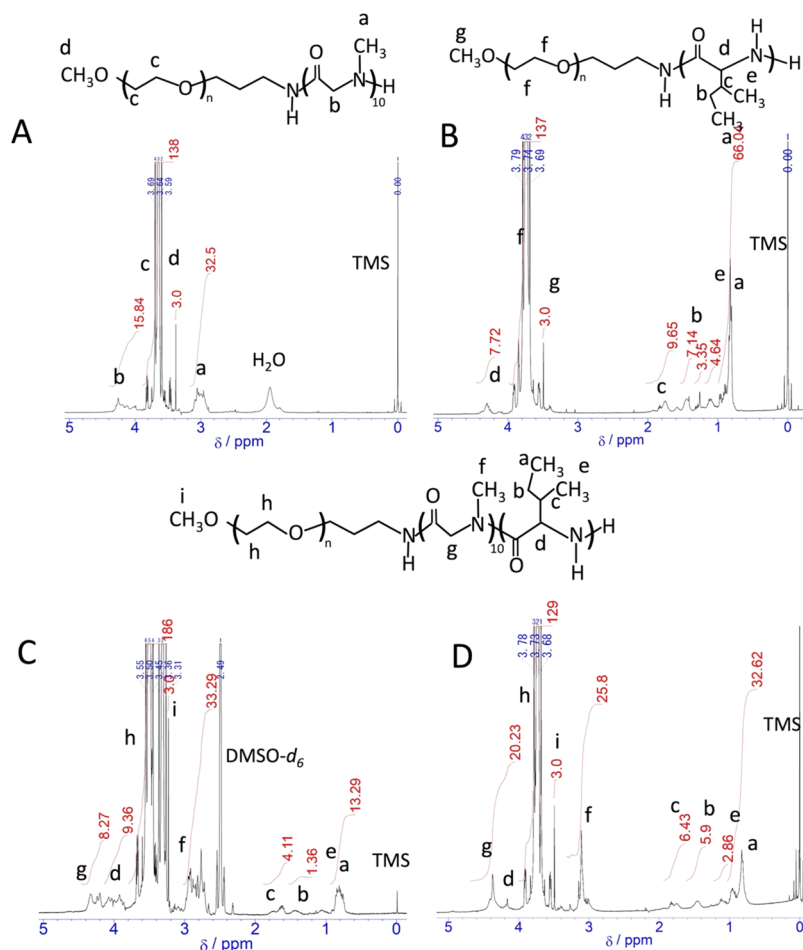


Figure 1. ^1H NMR spectra of (A) mPEG-P(Sar) $_n$ ($n = 10$) in CDCl_3 (0.5% v/v TFA), (B) mPEG-P(Ile) $_m$ ($m = 10$) in CDCl_3 (0.5% v/v TFA), (C) mPEG-P(Sar) $_n$ ($n = 11$)-P(Ile) $_m$ ($m = 5$) in $\text{DMSO}-d_6$, and (D) mPEG-P(Sar) $_n$ ($n = 11$)-P(Ile) $_m$ ($m = 5$) in CDCl_3 (0.5% v/v TFA).

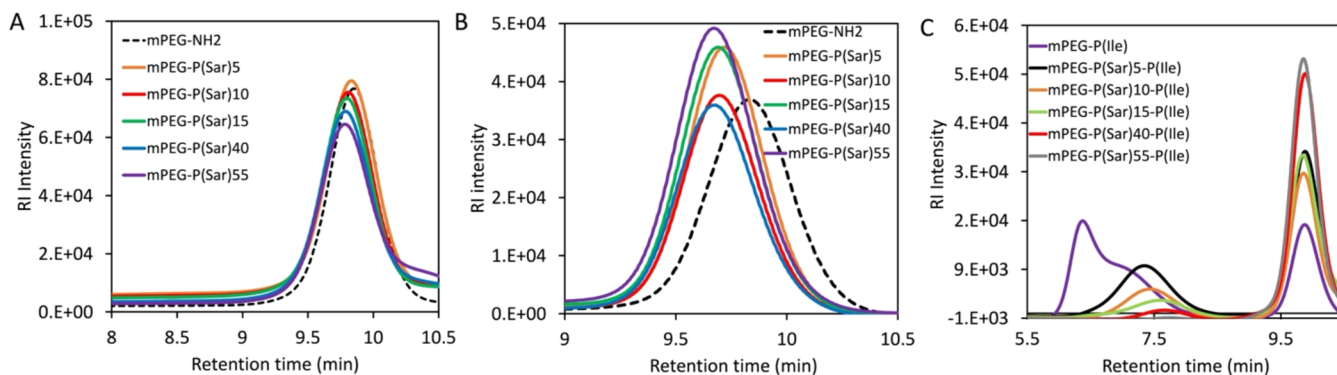


Figure 2. GPC charts of (A) mPEG-P(Sar) in D-PBS, (B) PEG-P(Sar) in DMF, and (C) mPEG-P(Ile) and mPEG-P(Sar)-P(Ile) in D-PBS. The sample concentration was 2.0 mg/mL.

min, and dissociation of polymers from antibodies was followed for 5 min.

3. RESULTS AND DISCUSSION

3.1. Synthesis and Characterization of Diblock and Triblock Copolymers. We prepared mPEG-P(Sar)s by means of mPEG-NH₂-initiated Sar-NCA ring-opening polymerization, and we characterized the obtained polymers by means of ^1H NMR. Table 1 summarizes the polymerization process. Figure 1A presents the ^1H NMR spectrum for PEG-P(Sar) (number of sarcosine units = 10). The number of

repeating units of sarcosine in PEG-P(Sar) was calculated by comparing the integral ratio of the PEG's methoxy terminal peak to the *N*-methyl group of sarcosine peak. We performed GPC to determine molecular weights, and the results reveal that all polymers exhibited a narrow unimodal M_w distribution peak (polydispersity index = 1.05) (Figure 2B). Moreover, the GPC peak shifted toward higher molecular weights due to the increase in the degree of polymerization of P(Sar). Importantly, we obtained various molecular weights of polymers by performing mPEG-NH₂-initiated Sar-NCA polymerization reactions. In addition, we synthesized mPEG-

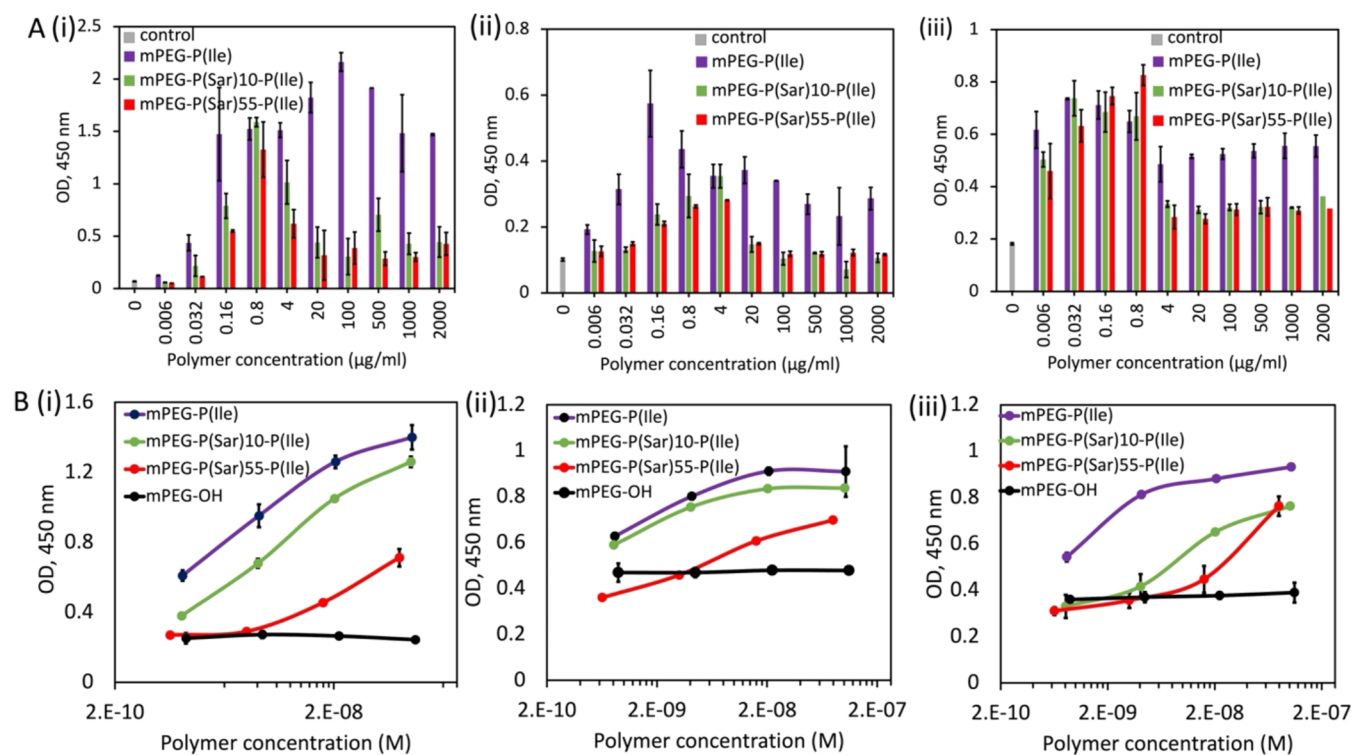
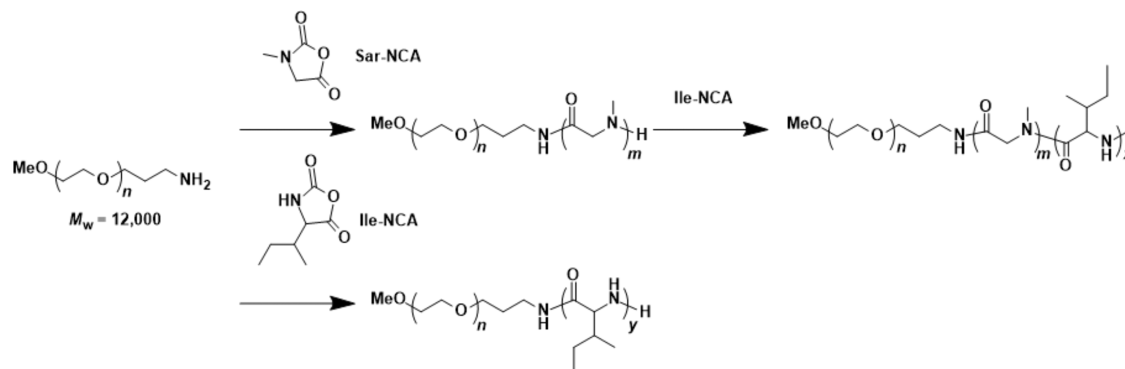
Scheme 1. Synthesis of Di- and Tri-copolymers *via* Ring-Opening NCA Polymerization

Figure 3. (A) Indirect ELISA results regarding the binding properties of (i) mIgG antibody 15–2b, (ii) mIgG antibody 6.3, and (iii) mIgM antibody AGP4 in relation to various concentrations of mPEG-P(Sar), mPEG-P(Ile), and mPEG-P(Sar)-P(Ile). (B) Sandwich ELISA results regarding the binding properties of (i) mIgG antibody 15–2b, (ii) mIgG antibody 6.3, and (iii) mIgM antibody AGP4 in relation to various concentrations of mPEG-P(Ile) and mPEG-P(Sar)-P(Ile). Control results were obtained on D-PBS treatment. Error bars represent standard deviation for duplicate measurements.

P(Ile) using mPEG-NH₂ as an initiator. We characterized mPEG-P(Ile) by means of ¹H NMR spectroscopy in CDCl₃ with TFA (Figure 1B). We determined the number of isoleucine units of mPEG-P(Ile) by comparing the integral ratio of the PEG's methoxy terminal peak to the isoleucine's two –CH₃ peaks at 0.90 ppm.

Next, we synthesized mPEG-P(Sar)-P(Ile) using mPEG-P(Sar) as a macroinitiator (Scheme 1). In order to determine the number of repeating units of sarcosine and isoleucine, we used DMSO-*d*₆ and CDCl₃ as NMR solvents, respectively. The ¹H NMR peak intensities of the *N*-methyl group for sarcosine units in the triblock copolymers were less apparent in CDCl₃ than in DMSO-*d*₆. We calculated the number of repeating units of sarcosine and isoleucine in the triblock copolymers from ¹H NMR in DMSO-*d*₆ and CDCl₃, respectively. As we expected, there were no obvious changes

in the number of sarcosine units (Figures 1C and S5). The calculated number of repeating units of isoleucine was in the range between 3.03 and 10.1. (Figures 1D and S6).

Figure 2 presents the GPC charts of both (A) mPEG-P(Sar) and (B) mPEG-P(Sar)-P(Ile) possessing different numbers of sarcosine units in D-PBS. The peak shifting at 9.83 min toward shorter retention time on increasing sarcosine units for mPEG-P(Sar)s was entirely due to the enhancement in the molecular weight (Figures 2A and S7), which was also consistent with the molecular weight calculated from ¹H NMR (Table 1). The fact that all of the PEG-P(Sar)s exhibited a single GPC peak indicates that in D-PBS, they took the form of unimers.

By contrast, mPEG-P(Ile) exhibited two retention times: one at 6.4 min and another at 9.8 min (Figure 2B). The fact that peak retention times ranged from 6.4 to 7.8 min for mPEG-P(Ile)s indicates that, in D-PBS, they took the form of

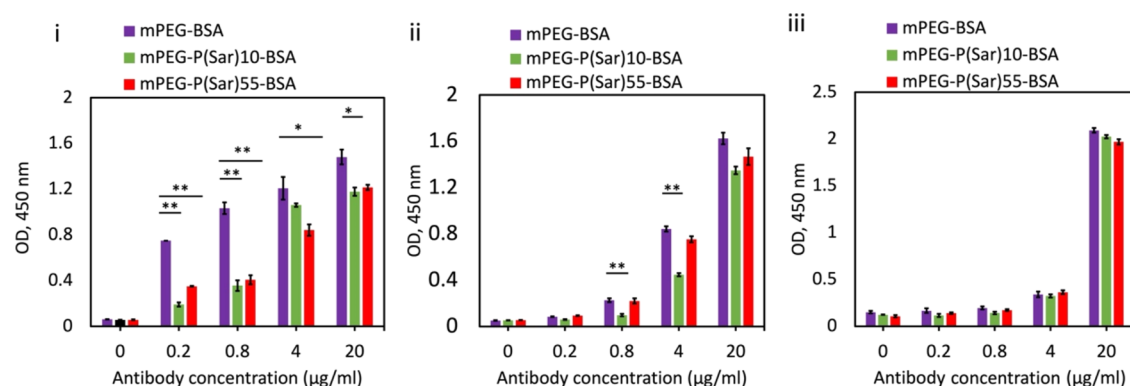


Figure 4. Indirect ELISA for binding of (i) mIgG antibody 15–2b, (ii) mIgG antibody 6.3, and (iii) mIgM antibody AGP4 with mPEG-BSA (20.0 µg/mL) or mPEG-P(Sar)-BSA (20.0 µg/mL)-immobilized plate wells. Statistical analysis for *P* values was calculated from Dunnett's test; ** indicates *p* < 0.001 and * indicates *p* < 0.05. Antibody concentration 0 indicates control data (D-PBS (–) treated). Error bars represent standard deviation for quadruplets measurement.

aggregates owing to the hydrophobicity of P(Ile). The peak corresponding to 6.4 min of retention time for mPEG-P(Ile) was delayed to the retention time (7.29 min) for the triblock copolymer, mPEG-P(Sar)5-P(Ile) (Table S4). Such consequences could be described as the effect of hydrophilicity of P(Sar) on hydrophobic P(Ile). Moreover, the impact of hydrophilicity was periodically predominated with increasing numbers of sarcosine as supported by GPC peak shifting to retention time (~7.64) (Table S4). Importantly, we found that mPEG-P(Sar)-P(Ile) possessing 55 sarcosine units exhibited a very small peak. Finally, it could be accomplished that hydrophilic P(Sar) has a true impact on the behavior of mPEG-P(Sar)-P(Ile).

3.2. Antibody Binding. In this study, we conducted binding assays of anti-PEG mAbs and mPEG-P(Sar)-P(Ile) to identify the latter's possible hydrophilic benefits of P(Sar). We confirmed the critical micelle concentration (CMC) of obtained polymers (Figure S7). The CMC of mPEG-P(Ile), mPEG-P(Sar)10-P(Ile), and mPEG-P(Sar)55-P(Ile) was determined to be 5×10^{-6} , 8×10^{-6} , and 1×10^{-5} M, respectively (Figure S7D). Specifically, we used three ELISA-based assays (the indirect ELISA assay, the sandwich ELISA assay, and the competitive ELISA assay) and biosensor-based BLI assay to assess the binding properties of three monoclonal anti-PEG Abs (mAbs)—the PEG main-chain-specific mIgM antibody AGP4, the PEG main-chain-specific mIgG antibody 6.3, and the terminal methoxy-specific mIgG antibody 15–2b—in relation to two distinctly PEG conjugates: mPEG-P(Ile), and mPEG-P(Sar)-P(Ile). We initially dissolved three mPEG conjugates in ethanol and then diluted them to different polymer concentrations in H₂O/ethanol (v/v = 1:1) for polymer coating (polymer concentration = 0.006 to 2000 µg/mL). The binding behaviors of three anti-PEG mAbs for three mPEG-conjugate-immobilized plates were envisaged by indirect ELISA. It should be noted that P(Ile), as a hydrophobic block was adsorbed on plate wells. The binding behavior was determined by the absorbance value, wherein high absorbance values would indicate effective binding. The binding behavior of all anti-PEG mAbs was dependent on the concentrations of the polymer coatings as well as the types of mPEG conjugates. Anti-PEG mAbs exhibited binding to mPEG-P(Ile) at a wide concentration range. The lowest binding at the lowest concentration suggested a smaller number of PEG on the plate wells. However, bindings of

anti-PEG Abs were proliferated with an increase in the concentration of both PEG-P(Ile) and mPEG-P(Sar)-P(Ile) due to an increase in the number of PEG on plates (concentration range, 0.006–0.8 µg/mL). However, at higher PEG concentrations (20.0–2000 µg/mL), the occupancy of P(Ile) on the hydrophobic plates of both PEG-P(Ile) and mPEG-P(Sar)-P(Ile) polymers was saturated (Figure 3A,i,ii,iii). We consider that coating of the PEG-polymers onto the plate wells saturated beyond the concentration of 20 µg/mL. Importantly, a sudden decline in binding for all antibody cases after a particular concentration was possibly due to the formation of a brush structure of PEGs onto the plate at a high mPEG-P(Ile) concentration.⁴⁷

Interestingly, the binding behavior of three anti-PEG mAbs was drastically minimized for P(Sar)-inserted mPEG-P(Sar)-P(Ile) triblock copolymers, as evidenced by steady suppression of binding (Figure 3A). Previously, we examined the binding behaviors of anti-PEG IgM in relation to both PEG-*b*-poly(aspartic acid)-*b*-poly(L-phenylalanine) (PEG-P(Asp)-P(Phe))-immobilized plates and PEG-PBLA-immobilized plates.³⁷ We observed that anti-PEG IgM did not bind well to PEG-P(Asp)-P(Phe), but bound effectively to PEG-PBLA. This observation indicated that anti-PEG IgM recognized PEG, and the bindings of anti-PEG IgM were induced by hydrophobic blocks and the surface at proximity of PEG. Owing to the haptenic characteristic of PEG, the hydrophobic blocks of the PEG conjugate helped anti-PEG IgM bind to the PEG. The binding behaviors of all three anti-PEG mAbs to the immobilized mPEG-P(Sar)-P(Ile) were much less pronounced than the immobilized mPEG-P(Ile) due to the presence of P(Sar) as a hydrophilic spacer. This indicates that the presence of the P(Sar) block clearly suppressed anti-PEG mAbs' bindings.

Figure 3B exhibits binding behaviors of mPEG-P(Ile) and mPEG-P(Sar)-P(Ile) to three types of anti-PEG mAbs-immobilized sandwich ELISA, and we examined sandwich ELISA far below the CMC of three polymers (Figure 3B). For all anti-PEG mAbs, binding levels were higher for mPEG-P(Ile) than for mPEG-P(Sar)-P(Ile). It should be noted that the binding level associated with mPEG-OH exhibited no change with concentration and were similar to the control result (Figure S8); this negligible binding tendency reflects the haptenic characteristic of PEG itself.⁴⁸ Despite having mPEG-OH specificity to anti-PEG mAbs, the affinity of mPEG-OH

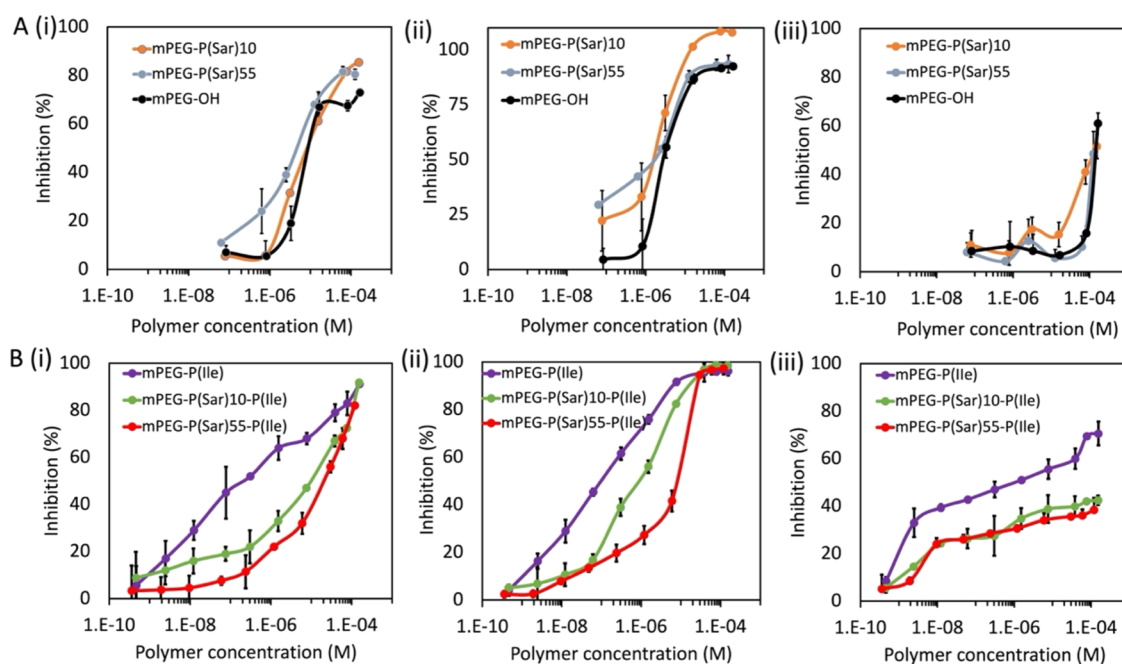


Figure 5. Competitive ELISA results of (i) mIgG antibody 15–2b (1.3×10^{-8} M), (ii) mIgG antibody 6.3 (3.3×10^{-8} M), and (iii) mIgM antibody AGP4 (2.1×10^{-9} M) in relation to various concentrations of (A) mPEG-OH and mPEG-P(Sar)s and (B) mPEG-P(Ile) and mPEG-P(Sar)-P(Ile). (Error bars represent the standard deviation for duplicate measurements.). Concentrations of antibodies were constant at 2.0 mg/mL.

was too weak to form a stable bound complex with anti-PEG mAbs in the solution.³⁸ Generally, bare PEG exhibits bioinert nature due to its hydrophilic and flexible properties.⁴⁹ However, all of the antibodies were able to bind to PEG possessing hydrophobic conjugates, as evidenced by the maximum binding of antibodies to mPEG-P(Ile). Although, both mPEG-P(Ile) and mPEG-P(Sar)-P(Ile) possess P(Ile), there was a drastic difference in binding propensity between mPEG-P(Ile) and mPEG-P(Sar)-P(Ile). Our findings in the current study suggest that hydrophobic blocks help the haptenic characteristic of PEG for stable bindings. Both the mIgG antibody, 6.3, and mIgM antibody, AGP4, recognized the PEG main chain; therefore, both antibodies weakly interacted with the haptenic PEG main chain. Although researchers have reported about the effects of the hydrophobicity of polymers on immunogenic proteins,³⁵ still there is a great deal of queries about the reason for the precise effects of the hydrophobic blocks of PEG conjugates on antibody binding. As we expected, P(Sar), when it was made part of the triblock copolymer mPEG-P(Sar)-P(Ile), effectively suppressed the ability of antibodies to bind to the copolymer. Moreover, mPEG-P(Sar)-P(Ile) possessing long P(Sar) blocks did a better job of suppressing the binding tendencies of antibodies than did mPEG-P(Sar)-P(Ile) possessing short P(Sar) blocks. Thus, we witnessed the maximum suppression of anti-PEG mAbs' binding to PEG when the maximum number of P(Sar) units (55) was present in the triblock copolymer, signifying the impact hydrophilic property of P(Sar) on PEG. Moreover, sandwich ELISA without an antibody at different concentrations of mPEG-P(Ile), mPEG-P(Sar)-P(Ile), and mPEG-OH is shown in Figure S9.

We examined the binding tendency of three anti-PEG mAbs: anti-PEG mAbs are terminal methoxy-specific anti-PEG mIgG (mIgG antibody 15–2b), PEG main-chain-specific mIgG (mIgG antibody 6.3), and PEG main-chain-specific mIgM

(mIgM antibody AGP4). Figure 4 exhibits concentration-dependent binding tendency of anti-PEG mAbs with polymer conjugates including mPEG-BSA or mPEG-P(Sar)-BSA. In our careful experiment, we clearly observed the difference in binding for mPEG-BSA and mPEG-P(Sar)-BSA with anti-PEG IgG (15–2b, and 6.3, Figure 4,i,ii), which possess a low molecular weight as compared to IgM (AGP4). In general, IgG is a more antigen-specific antibody than IgM, but IgM can bind with low specificity. Probably, due to the larger molecular weight and low specificity of AGP4, it preferred to bind with polymer nonspecifically. Therefore, in the case of AGP4, the binding difference for different polymers was not noticed (Figure 4,iii). Furthermore, we confirmed the significant difference in binding for mPEG-BSA and mPEG-P(Sar)-BSA with anti-PEG antibodies. The significant difference in the obtained *p* values indicates the effect of P(Sar) in mPEG-P(Sar)-BSA on suppression of antibody binding. However, at a high concentration of an antibody, the difference in binding for mPEG-BSA and mPEG-P(Sar)-BSA with anti-PEG antibodies was small, probably due to the occurrence of bindings between the added antibody and the antibody-PEG-bound complex.

We performed competitive ELISA with mPEG-OH, and two mPEG-P(Sar)s: mPEG-P(Sar)10 and mPEG-P(Sar)55. For this test, we premixed the antibodies with PEG conjugates and added the obtained solution to mPEG-immobilized wells. A relatively high concentration of mPEG-OH was required to inhibit the binding of all of the antibodies. Importantly, the inhibiting effects of mPEG-P(Sar)s were similar to those of mPEG-OH (Figure 5A). Although anti-PEG-mAbs are specific to the PEG main-chain group and to the terminal methoxy group, results indicated that the binding of anti-PEG mAbs to each specific region of PEG was not strong enough, as evidenced by different half maximal inhibitory concentrations (IC_{50}) for both mPEG-OH and mPEG-P(Sar)s (Table S5). In contrast to this competitive ELISA, mIgG antibody 15–2b,

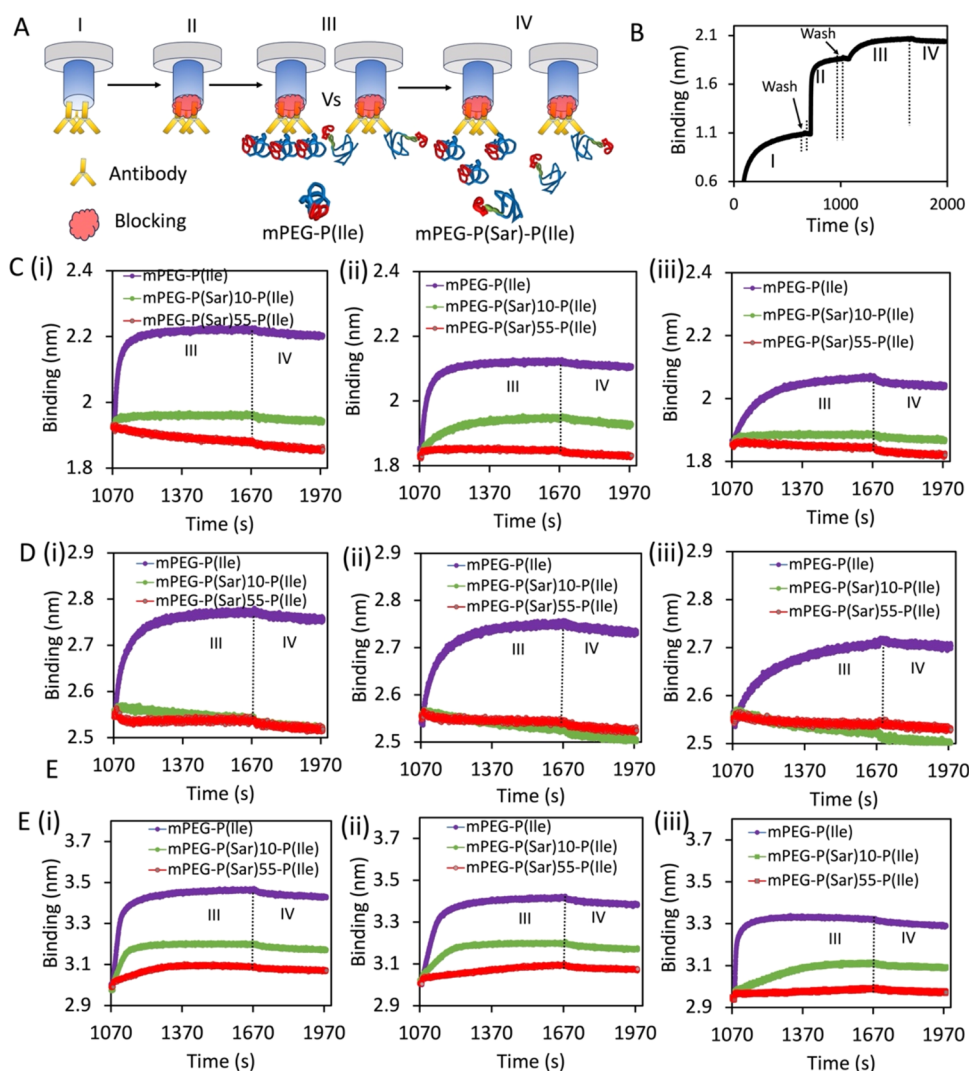


Figure 6. (A) Schematic presentation of the BLI assay experiment. (B) Binding signals for each step in our BLI assay. BLI assay for different polymers to (C) mIgG antibody 15–2b, (D) mIgG antibody 6.3, and (E) mIgM antibody AGP4. Concentration of polymers: (i) 2×10^{-6} M, (ii) 1×10^{-6} M, and (iii) 5×10^{-7} M.

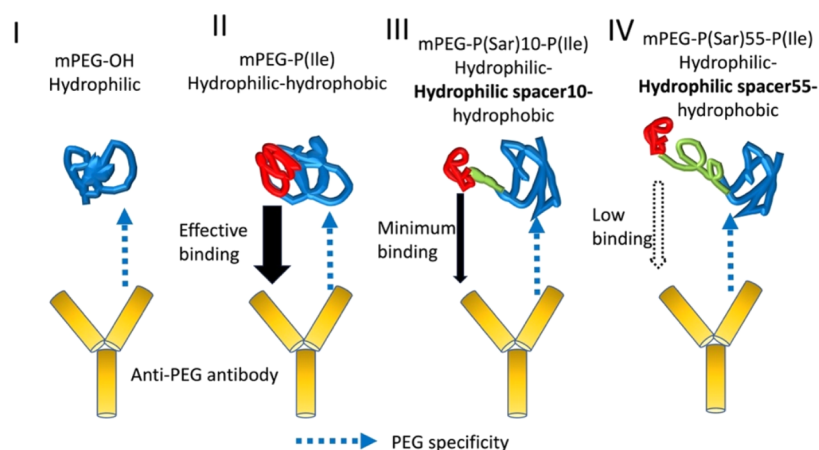
mIgG antibody 6.3, and mIgM antibody AGP4 were sharply inhibited by P(Ile) block-conjugated diblock copolymers, mPEG-P(P(Ile)) (Figure 5B). Likewise indirect and sandwich ELISA, bindings of anti-PEG mAbs were suppressed by mPEG-P(Sar)-P(Ile)s. Thus, a substantial difference in anti-PEG antibody inhibition between mPEG-P(Ile) and mPEG-P(Sar)-P(Ile) was prominent. Notably, a relatively low IC₅₀ of mPEG-P(Ile) indicated its higher inhibiting potency to three anti-PEG mAbs than other polymers (Table S5). As we examined the effects that the insertion of the P(Sar) block into mPEG-P(Ile) had on the binding behaviors of anti-PEG mAbs, we noted that P(Sar) seems to play the main role: it keeps PEGs separated from hydrophobic P(Ile) blocks.

In the inhibition ELISA, inhibitory effects of PEG-P(Sar) were nearly the same as that of mPEG-OH (Figure 5A). In addition, similar binding behaviors of PEG and PEG-P(Sar) were also supported by sandwich ELISA. (Data are not shown). It has been known that PEG itself does not show immunogenicity. Therefore, based on both competitive and sandwich ELISA results, we have assumed that no or little difference in PEG's immunogenic property between PEG and

PEG-P(Sar) will be found in our future immunogenicity assessment study.

The BLI is a biosensor-based dip-and-read platform that dips biosensors into designated plate wells to perform each step. In order to conduct antibody binding with the polymers, we followed mainly four steps (Figure 6A,B). First, immobilization of the antibody on the sensors (antibody loading step) (I), blocking of sensors (II), polymer binding step (association step) (III), and, finally, the removal of unbound polymers (dissociation step) (IV). The binding of polymers to antibody-immobilized sensors was examined by analyzing different concentrations of mPEG-P(Ile) and mPEG-P(Sar)-P(Ile) at their below CMC. However, we observed stark contrasts between mPEG-P(Ile) and mPEG-P(Sar)-P(Ile). The associative behavior of mPEG-P(Sar)-P(Ile) to all of the anti-PEG mAbs was notably lower than that of mPEG-P(Ile) at the same concentration of the polymers. The association of mPEG-P(Sar)-P(Ile) to anti-PEG mAbs-immobilized sensors was greatly suppressed by the triblock copolymer with a long P(Sar) chain length in all antibody cases (Figure 6C–E). We also confirmed that mPEG-OH exhibited negligible changes in the same concentration range (Figure

Scheme 2. Schematic of the Effective Binding of mPEG-P(Ile) with an Anti-PEG Antibody and the Suppression of Binding for mPEG-P(Sar)-P(Ile)



S10). Therefore, the results indicated P(Sar)-chain-length-dependent suppression, signifying the role of P(Sar) in between mPEG and P(Ile).

It is considered that hydrophobic blocks adjoining to PEG chains are highly affected by anti-PEG Abs. In PEG-liposome cases, lipid membranes are adjoining to short PEG (2k) chains; therefore, it is also considered that the lipid membranes greatly contribute for anti-PEG mAbs' bindings.⁵⁰ Furthermore, the mushroom formation of the short PEG chain may also be due to hydrophobic lipid membranes.⁵¹ A study found that an injection of 40k free PEG, 30 min prior to administrating in mice, suppressed the PEG-liposome-induced elicitation of anti-PEG IgM.⁵² This result indicated that high-molecular-weight 40k PEG, even though it is more hydrophobic than low-molecular-weight PEG, did not elicit an anti-PEG IgM response. Recently, Yuan et al. evaluated about the positive impact of hidden hydrophobicity on the hydrophilic polymer in relation to polymer conjugation to highly immunogenic proteins.³⁵ Therefore, it could be considered that hydrophobic blocks adjoining PEG chains play a pivotal role in effective binding with anti-PEG mAbs. Anti-PEG mAbs interact with PEGs due to their PEG specificity, but their interactions are not strong enough. This was supported by a negligible binding of mPEG-OH with anti-PEG mAbs in our current experiments. (Scheme 2,I) However, anti-PEG mAbs exhibited bindings to mPEG-P(Ile), in which mPEG was conjugated with hydrophobic blocks, P(Ile) (Scheme 2,II). Importantly, the insertion of hydrophilic P(Sar) into mPEG-P(Ile) significantly suppressed anti-PEG mAbs' bindings, indicating the pivotal role of hydrophilic P(Sar) for suppression of anti-PEG mAbs' bindings (Scheme 2,III,IV). As a hydrophilic polymer, P(Sar) separates the PEG from the hydrophobic P(Ile) block so that PEG exhibits truly haptenic behaviors.

4. CONCLUSIONS

We have successfully synthesized a series of double hydrophilic block copolymers, mPEG-P(Sar), in which P(Sar) preserved the intrinsic hydrophilic nature of PEG. We observed that the behavior of mPEG-P(Sar) in aqueous solutions was similar to the behavior of PEG in aqueous media. Moreover, we observed that the hydrophilicity of P(Sar) enhanced the hydrophilic ability of mPEG-P(Sar)-P(Ile) to reduce the level of aggregation of the triblock copolymers inserted with P(Sar). In the current study, we examined various types of anti-PEG

mAbs binding to three types of polymers, including mPEG, mPEG-P(Sar), and mPEG-P(Sar)-P(Ile). The terminal methoxy group-specific antibody, mIgG antibody 15–2b, exhibited distinct binding from those of the main-chain-specific antibodies, mIgG antibody 6.3 or mIgM antibody AGP4. Importantly, we found that the hydrophilicity of P(Sar) preserved the hydrophilicity of PEG. Therefore, our findings strongly support our proof of concept that P(Sar) could effectively inhibit the stable bindings of anti-PEG mAbs to PEGs in the mPEG-hydrophobic conjugate. Overall, the results of our present study suggest that P(Sar) has a significant role in suppression of anti-PEG mAbs' bindings to PEG-hydrophobic conjugates. We have high expectations that mPEG-P(Sar) can be an effective or even superior alternative to PEG as a protein shield capable of minimizing the immunogenicity of PEGylated proteins. Thus, we encourage researchers in the field to conduct future *in vivo* studies on the topic.

■ ASSOCIATED CONTENT

SI Supporting Information

The Supporting Information is available free of charge at <https://pubs.acs.org/doi/10.1021/acsomega.4c02655>.

Additional results including ¹H NMR, FTIR, GPC, antibody binding, and BLI (PDF)

■ AUTHOR INFORMATION

Corresponding Author

Kouichi Shiraishi – Research Center for Medical Sciences, The Jikei University School of Medicine, Kashiwa, Chiba 277-0004, Japan; orcid.org/0009-0003-5097-4567; Email: kshiraishi@jikei.ac.jp

Authors

Debabrata Maiti – Research Center for Medical Sciences, The Jikei University School of Medicine, Kashiwa, Chiba 277-0004, Japan; orcid.org/0000-0002-3912-5762

Masayuki Yokoyama – Research Center for Medical Sciences, The Jikei University School of Medicine, Kashiwa, Chiba 277-0004, Japan; orcid.org/0000-0001-6053-1856

Complete contact information is available at: <https://pubs.acs.org/10.1021/acsomega.4c02655>

Notes

The authors declare no competing financial interest.

ACKNOWLEDGMENTS

This study was supported by JSPS KAKENHI Grant-in-Aid for Transformative Research Areas (A) (Grant Number 20H05875).

REFERENCES

- (1) Suk, J. S.; Xu, Q.; Kim, N.; Hanes, J.; Ensign, L. M. PEGylation as a strategy for improving nanoparticle-based drug and gene delivery. *Adv. Drug Delivery Rev.* **2016**, *99*, 28–51.
- (2) Armstrong, J. K.; Hempel, G.; Koling, S.; Chan, L. S.; Fisher, T.; Meiselman, H. J.; Garratty, G. Antibody against poly(ethylene glycol) adversely affects PEG-asparaginase therapy in acute lymphoblastic leukemia patients. *Cancer* **2007**, *110*, 103–111.
- (3) Hershfield, M. S.; Ganson, N. J.; Kelly, S. J.; Scarlett, E. L.; Jagers, D. A.; Sundry, J. S. Induced and pre-existing anti-polyethylene glycol antibody in a trial of every 3-week dosing of pegloticase for refractory gout, including in organ transplant recipients. *Arthritis Res. Ther.* **2014**, *16*, No. R63.
- (4) Barenholz, Y. C. Doxil—the first FDA-approved nano-drug: lessons learned. *J. Controlled Release* **2012**, *160* (2), 117–134.
- (5) Zhang, H. Onivyde for the therapy of multiple solid tumors. *OncoTargets Ther.* **2016**, *9*, 3001–3007.
- (6) Yang, Z.; Chen, H. The recent progress of inorganic-based intelligent responsive nanopatform for tumor theranostics. *View* **2023**, *3* (6), No. 20220009.
- (7) Zhu, Y.; Li, Q.; Wang, C.; Hao, Y.; Yang, N.; Chen, M.; Ji, J.; Feng, L.; Liu, Z. Rational design of biomaterials to potentiate cancer thermal therapy. *Chem. Rev.* **2023**, *123* (11), 7326–7378.
- (8) Anselmo, A. C.; Mitragotri, S. A review of clinical translation of inorganic nanoparticles. *AAPS J.* **2015**, *17*, 1041–1054.
- (9) Chen, B. M.; Cheng, T. L.; Roffler, S. R. Polyethylene glycol immunogenicity: theoretical, clinical, and practical aspects of anti-polyethylene glycol antibodies. *ACS Nano* **2021**, *15* (9), 14022–14048.
- (10) Ibrahim, M.; Shimizu, T.; Ando, H.; Ishima, Y.; Elgarhy, O. H.; Sarhan, H. A.; Hussein, A. K.; Ishida, T. Investigation of anti-PEG antibody response to PEG-containing cosmetic products in mice. *J. Controlled Release* **2023**, *354*, 260–267.
- (11) Elsadek, N. E.; Lila, A. S.; Ishida, T. Immunological Responses to PEGylated Proteins: Anti-PEG Antibodies. In *Polymer-Protein Conjugates*; Elsevier, 2020; pp 103–123.
- (12) Mohamed, M.; Lila, A. S. A.; Shimizu, T.; Alaaeldin, E.; Hussein, A.; Sarhan, H. A.; Szebeni, J.; Ishida, T. PEGylated liposomes: immunological responses. *Sci. Technol. Adv. Mater.* **2019**, *20*, 710–724.
- (13) Liu, M.; Chu, Y.; Liu, H.; Su, Y.; Zhang, Q.; Jiao, J.; Liu, M.; Ding, J.; Liu, M.; Hu, Y.; Dai, Y.; Zhang, R.; Liu, X.; Deng, Y.; Song, Y. Accelerated blood clearance of nanoemulsions modified with PEG-cholesterol and PEG-phospholipid derivatives in rats: the effect of PEG-lipid linkages and PEG molecular weights. *Mol. Pharmaceutics* **2020**, *17* (4), 1059–1070.
- (14) Mima, Y.; Hashimoto, Y.; Shimizu, T.; Kiwada, H.; Ishida, T. Anti-PEG IgM is a major contributor to the accelerated blood clearance of polyethylene glycol-conjugated protein. *Mol. Pharmaceutics* **2015**, *12* (7), 2429–2435.
- (15) Zhang, Z.; Chu, Y.; Li, C.; Tang, W.; Qian, J.; Wei, X.; Lu, W.; Ying, T.; Zhan, C. Anti-PEG scFv corona ameliorates accelerated blood clearance phenomenon of PEGylated nanomedicines. *J. Controlled Release* **2021**, *330*, 493–501.
- (16) Kozma, G. T.; Mešzaáros, T.; Vashegyi, I.; Fülöp, T.; Örfi, E.; Dežsi, L.; Rosivall, L.; Bavli, Y.; Urbanics, R.; Mollnes, T. E.; Barenholz, Y.; Szebeni, J. Pseudo-anaphylaxis to polyethylene glycol (PEG)-coated liposomes: roles of anti-PEG IgM and complement activation in a porcine model of human infusion reactions. *ACS Nano* **2019**, *13*, 9315–9324.
- (17) Shimizu, T.; Awata, M.; Lila, A. S. A.; Yoshioka, C.; Kawaguchi, Y.; Ando, H.; Ishima, Y.; Ishida, T. Complement activation induced by PEG enhances humoral immune responses against antigens encapsulated in PEG-modified liposomes. *J. Controlled Release* **2021**, *329*, 1046–1053.
- (18) Gabizon, A.; Szebeni, J. Complement activation: a potential threat on the safety of poly(ethylene glycol)-coated nanomedicines. *ACS Nano* **2020**, *14* (7), 7682–7688.
- (19) Chen, E.; Chen, B. M.; Su, Y. C.; Chang, Y. C.; Cheng, T. L.; Barenholz, Y.; Roffler, S. R. Premature drug release from polyethylene glycol (PEG)-coated liposomal doxorubicin via formation of the membrane attack complex. *ACS Nano* **2020**, *14* (7), 7808–7822.
- (20) Quach, H. Q.; Kong, R. L. X.; Kah, J. C. Y. Complement activation by PEGylated gold nanoparticles. *Bioconjugate Chem.* **2018**, *29* (4), 976–981.
- (21) Ibrahim, M.; Shimizu, T.; Ando, H.; Ishima, Y.; Elgarhy, O.; Elgarhy, O. H.; Sarhan, H. A.; Hussein, A. K.; Ishida, T. Investigation of anti-PEG antibody response to PEG-containing cosmetic products in mice. *J. Controlled Release* **2023**, *354*, 260–267.
- (22) Chen, B. M.; Su, Y. C.; Chang, C. J.; Burnouf, P. A.; Chuang, K. H.; Chen, C. H.; Cheng, T. L.; Chen, Y. T.; Wu, J. Y.; Roffler, S. R. Measurement of Pre-Existing IgG and IgM Antibodies against Polyethylene Glycol in Healthy Individuals. *Anal. Chem.* **2016**, *88* (88), 10661–10666.
- (23) Hsieh, Y. C.; Wang, H. E.; Lin, W. W.; Roffler, S. R.; Cheng, T. C.; Su, Y. C.; Li, J. J.; Chen, C. C.; Huang, C. H.; Chen, B. M.; Wang, J. Y.; Cheng, T. L.; Chen, F. M. Pre-existing anti-polyethylene glycol antibody reduces the therapeutic efficacy and pharmacokinetics of PEGylated liposomes. *Theranostics* **2018**, *8* (8), 3164–3175.
- (24) Povsic, T. J.; Lawrence, M. G.; Lincoff, A. M.; Mehran, R.; Rusconi, C. P.; Zelenkofske, S. L.; Huang, Z.; Sailstad, J.; Armstrong, P. W.; Steg, G.; Bode, C.; Becker, R. C.; Alexander, J. H.; Adkinson, N. F.; Levinson, A. I. Pre-existing anti-PEG antibodies are associated with severe immediate allergic reactions to pegnivacogin, a PEGylated aptamer. *J. Allergy Clin. Immunol.* **2016**, *138* (6), 1712–1715.
- (25) Sellaturay, P.; Nasser, S.; Islam, S.; Gurugama, P.; Ewan, P. W. Polyethylene glycol (PEG) is a cause of anaphylaxis to the Pfizer/BioNTech mRNA COVID-19 vaccine. *Clin. Exp. Allergy* **2021**, *51* (6), 861–863.
- (26) Yao, X.; Qi, C.; Sun, C.; Huo, F.; Jiang, X. Poly(ethylene glycol) alternatives in biomedical applications. *Nano Today* **2023**, *48*, No. 101738.
- (27) d'Arcy, R.; Mohtadi, F. E.; Francini, N.; DeJulius, C. R.; Back, H.; Gennari, A.; Geven, M.; Cavestany, M. L.; Turhan, Z. Y.; Yu, F.; Lee, J. B.; King, M. R.; Kagan, L.; Duvall, C. L.; Tirelli, N. A Reactive Oxygen Species-Scavenging ‘Stealth’ Polymer, Poly(thioglycidyl glycerol), Outperforms Poly(ethylene glycol) in Protein Conjugates and Nanocarriers and Enhances Protein Stability to Environmental and Biological Stressors. *J. Am. Chem. Soc.* **2022**, *144* (46), 21304–21317.
- (28) Li, B.; Yuan, Z.; Jain, P.; Hung, H. C.; He, Y.; Lin, X.; McMullen, P.; Jiang, S. De novo design of functional zwitterionic biomimetic material for immunomodulation. *Sci. Adv.* **2020**, *6* (22), No. eaba0754.
- (29) Zhang, P.; Sun, F.; Tsao, C.; Jiang, S.; et al. Zwitterionic gel encapsulation promotes protein stability, enhances pharmacokinetics, and reduces immunogenicity. *Proc. Natl. Acad. Sci. U.S.A.* **2015**, *112* (39), 12046–12051.
- (30) Li, B.; Jain, P.; Ma, J.; Smith, J. K.; Yuan, Z.; Hung, H. C.; He, Y.; Lin, X.; Wu, K.; Pfaendtner, J.; Jiang, S. Trimethylamine N-oxide-derived zwitterionic polymers: A new class of ultralow fouling bioinspired materials. *Sci. Adv.* **2019**, *5* (6), No. eaaw9562.
- (31) Hou, Y.; Zhou, Y.; Wang, H.; Sun, J.; Wang, R.; Sheng, K.; Yuan, J.; Hu, Y.; Chao, Y.; Liu, Z.; Lu, H. Therapeutic Protein PEPylation: the Helix of Nonfouling Synthetic Polypeptides Minimizes the Anti-Drug Antibody Generation. *ACS Cent. Sci.* **2019**, *5*, 229–236.
- (32) Liu, M.; Li, J.; Zhao, D.; Yan, N.; Zhang, H.; Liu, M.; Tang, X.; Hu, Y.; Ding, J.; Zhang, N.; Liu, X.; Deng, Y.; Song, Y.; Zhao, X.

Branched PEG-modification: A new strategy for nanocarriers to evade the accelerated blood clearance phenomenon and enhance anti-tumor efficacy. *Biomaterials* **2022**, *283*, No. 121415.

(33) Shin, K.; Suh, H. W.; Grundler, J.; Lynn, A. Y.; Pothupitiya, J. U.; Moscato, Z. M.; Reschke, M.; Bracaglia, L. G.; Daspit, A. S. P.; Saltzman, W. M. Polyglycerol and Poly(ethylene glycol) exhibit different effects on pharmacokinetics and antibody generation when grafted to nanoparticle surfaces. *Biomaterials* **2022**, *287*, No. 121676.

(34) Qiao, R.; Fu, C.; Li, Y.; Qi, X.; Ni, D.; Nandakumar, A.; Siddiqui, G.; Wang, H.; Zhang, Z.; Wu, T.; Zhong, J.; Tang, S. Y.; Pan, S.; Zhang, C.; Whittaker, M. R.; Engle, J. W.; Creek, D. J.; Caruso, F.; Ke, P. C.; Cai, W.; Whittaker, A. K.; Davis, T. P. Sulfoxide-Containing Polymer-Coated Nanoparticles Demonstrate Minimal Protein Fouling and Improved Blood Circulation. *Adv. Sci.* **2020**, *7* (13), No. 2000406.

(35) Yuan, Z.; McMullen, P.; Luozhong, S.; Sarker, P.; Tang, C.; Wei, T.; Jiang, S. Hidden hydrophobicity impacts polymer immunogenicity. *Chem. Sci.* **2023**, *14*, 2033–2039.

(36) Harris, J. M.; Chess, R. B. Effect of PEGylation on pharmaceuticals. *Nat. Rev. Drug Discovery* **2003**, *2*, 214–221.

(37) Shiraishi, K.; Kawano, K.; Maitani, Y.; Aoshi, T.; Ishii, K.; Sanada, Y.; Mochizuki, S.; Sakurai, K.; Yokoyama, M. Exploring the relationship between anti-PEG IgM behaviors and PEGylated nanoparticles and its significance for accelerated blood clearance. *J. Controlled Release* **2016**, *234*, 59–67.

(38) Shiraishi, K.; Hamano, M.; Ma, H.; Kawano, K.; Maitani, Y.; Aoshi, T.; Ishii, K. J.; Yokoyama, M. Hydrophobic blocks of PEG-conjugates play a significant role in the accelerated blood clearance (ABC) phenomenon. *J. Controlled Release* **2013**, *165* (3), 183–190.

(39) Bi, D.; Unthan, D. M.; Hu, L.; Bussmann, J.; Remaut, K.; Barz, M.; Zhang, H. Polysarcosine-based lipid formulations for intracranial delivery of mRNA. *J. Controlled Release* **2023**, *356*, 1–13.

(40) Xuan, S.; Gupta, S.; Li, X.; Bleuel, M.; Schneider, G. J.; Zhang, D. Synthesis and characterization of well-defined PEGylated polypeptoids as protein-resistant polymers. *Biomacromolecules* **2017**, *18*, 951–964.

(41) Singhai, M.; Bhattacharya, S. Polysarcosine: the best alternative of poly(ethylene glycol). *Curr. Appl. Polym. Sci.* **2021**, *4* (2), 93–98.

(42) England, R. M.; Moss, J. I.; Gunnarsson, A.; Parker, J. S.; Ashford, M. B. Synthesis and characterization of dendrimer-based polysarcosine star polymers: well-defined, versatile platforms designed for drug-delivery applications. *Biomacromolecules* **2020**, *21* (8), 3332–3341.

(43) Lv, R. K.; Qian, Z. Z.; Zhao, X. P.; Xiong, F.; Xu, Y. J.; Fan, W. P.; Yao, X. K.; Huang, W. Self-assembly of polysarcosine amphiphilic polymers-tethered gold nanoparticles for precise photo-controlled synergistic therapy. *Nano. Res.* **2023**, *16*, 5685–5694.

(44) Hu, Y.; Hou, Y.; Wang, H.; Lu, H. Polysarcosine as an alternative to PEG for therapeutic protein conjugation. *Bioconjugate Chem.* **2018**, *29* (7), 2232–2238.

(45) Bleher, S.; Buck, J.; Muhl, C.; Sieber, S.; Barnert, S.; Witzgmann, D.; Huwyler, J.; Barz, M.; Süss, R. Poly(Sarcosine) Surface Modification Imparts Stealth-Like Properties to Liposomes. *Small* **2019**, *15*, No. 1904716.

(46) Sun, J.; Chen, J.; Sun, Y.; Hou, Y.; Liu, Z.; Lu, H. On the origin of the low immunogenicity and biosafety of a neutral α -helical polypeptide as an alternative to polyethylene glycol. *Bioact. Mater.* **2024**, *32*, 333–343.

(47) Li, M.; Jiang, S.; Simon, J.; Frey, D. P.; M, L.; Wagner, M. L.; Mailänder, V.; Crespy, D.; Landfester, K. Brush Conformation of Polyethylene Glycol Determines the Stealth Effect of Nanocarriers in the Low Protein Adsorption Regime. *Nano Lett.* **2021**, *21* (4), 1591–1598.

(48) Zhang, P.; Sun, F.; Liu, S.; Jiang, S. Anti-PEG antibodies in the clinic: Current issues and beyond PEGylation. *J. Controlled Release* **2016**, *244*, 184–193.

(49) Abe, K.; Higashi, K.; Watabe, K.; Kobayashi, A.; Limwikrant, W.; Yamamoto, K.; Moribe, K. Effects of the PEG molecular weight of

a PEG-lipid and cholesterol on PEG chain flexibility on liposome surfaces. *Colloids Surf., A* **2015**, *474*, 63–70.

(50) Shiraishi, K.; Yokoyama, M. Toxicity and immunogenicity concerns related to PEGylated-micelle carrier systems: a review. *Sci. Technol. Adv. Mater.* **2019**, *20*, 324–336.

(51) Sherman, M. R.; Williams, L. D.; Sobczyk, M. A.; Michaels, S. J.; Saifer, M. G. P. Role of the methoxy group in immune responses to mPEG-protein conjugates. *Bioconjugate Chem.* **2012**, *23*, 485–499.

(52) McSweeney, M. D.; Shen, L.; DeWalle, A. C.; Joiner, J. B.; Ciociola, E. C.; Raghuvanshi, D.; Macauley, M. S.; Lai, S. K. Pre-treatment with high molecular weight free PEG effectively suppresses anti-PEG antibody induction by PEG-liposomes in mice. *J. Controlled Release* **2021**, *329*, 774–781.